Study on Kinetic Characteristics of Krypton and Xenon radioactive source term in molten salt reactor

Bo Zhou[1,2], *Rui* Yan[2,*], *Xiaohan* Yu[2], *Yang* Zou[2], *Shihe* Yu[2], *Pu* Yang[2], and *Yafen* Liu[2]

[1]University of Chinese Academy of Sciences, Beijing 100049, China
[2]Shanghai Institute of Applied Physics, Chinese Academy of Sciences, Shanghai 201800, China

Abstract. A numerical simulation program for the dynamic distribution of krypton and xenon with flow and on-line removal function was established for primary loop system of molten salt reactor(MSR) Based on Mathematica7.0.The simulation results of the static burnup was compared with ORIGEN-S program, and the deviation is less than 10%, which is in good agreement.The distribution and dynamic characteristics of krypton and xenon in the primary loop system were analyzed under the flow regionalization and online removal model.The results show that,the static burnup model underestimates the total ^{135}Xe activity about 6.61% in the system, and the total activity of krypton and xenon in the system is underestimated by about 1.46%.Under the maximum removal fraction, the total activity of krypton and xenon in the exhaust gas system is 1.84×10^{16}Bq, of which ^{83m}Kr, ^{85m}Kr, ^{87}Kr, ^{88}Kr, ^{133}Xe, ^{135}Xe and ^{138}Xe account for about 95.6%.The total activity of krypton and xenon in the primary loop system is 2.64×10^{14}Bq, of which ^{138}Xe, ^{135m}Xe, ^{134m}Xe, ^{87}Kr and ^{83m}Kr account for about 93.6%.The numerical simulation method and the conclusion consistent with the actual physical laws.Dynamic distribution, evolution and migration characteristics of krypton, xenon and these precursor in the primary loop in the molten salt can be simulated more accurately compared to static burnup model.The analysis results can provide a theoretical basis for the management scheme of airborne source termsthe cooling design of the radioactive exhaust system and the source term analysis in accident conditions for the molten salt reactor.

1 Introduction

The concept of Molten Salt Reactor (MSR) originated from the Aircraft Reactor Experiment (ARE)[1, 2] Molten Salt Reactor Experiment (MSRE)[3, 4], Molten Salt Breeding Reactor (MSBR) constructed or designed by Oak Ridge National Laboratory (ORNL) in the 1950s and 1970s[5, 6], Denatured Molten Salt Reactor (DMSR)[7] and other experimental reactors.In 2011, the Thorium-based Molten Salt Reactor Nuclear Energy System (TMSR) project was set up by Chinese Academy of Sciences. A molten salt reactor with 2 MW thermal power(Hereinafter referred to as 2MW MSR) is planned to be built in 2020[8].

krypton and xenon are strictly controlled emission sources of nuclear power plants. In the 2MW MSR, krypton and xenon will be blown into the off-gas system by the bubbling system at the pumping bowl. In order to ensure that the emissions of krypton and xenon meet the regulatory requirements, krypton and xenon need to be fully decayed in the off-gas system.The decay time and cooling system design are related to the total activity of the krypton and xenon blown into the off-gas system.The core fission product analysis program used in the engineering design of 2MW MSR is ORIGEN-S. The flow characteristics and spatial distribution of the krypton and xenon in primary loop of molten salt reactor can not be analyzed by such a static burnup program.So, a fission products source term analysis program for the primary loop and off-gas system of molten salt reactor was established and preliminarily validated with reference program ORIGEN-S based on Mathematica 7.0 program. Then, the krypton and xenon distribution in the primary loop system and off-gas system of 2MW MSR under the flow state was calculated.

2 Model and Method

The SCALE program was used to calculate neutron flux and energy spectrum parameters. The ORIGEN-S program in SCALE package was used to calculate the production of the krypton and xenon as a comparison with this work. The calculation model is shown in figure 1 and figure 2. The core diameter and height are 190 cm and 180 cm respectively. ASME-N10003 nickel-based alloy material is used in the main container and metal support structure of the reactor core, and graphite is used as moderator material. Control rods, experimental and measuring devices and neutron sources are arranged in 11 functional channels. No.1, No.2, No.3, No.4, No.5, No.6 are control rod channels, No.7 is neutron source channels, No.8, No.9, No.10, No.11 are irradiation experimental and measurement channels. The design parameters(conceptual design stage)and the Schematic diagram of the primary loop system are shown in Table 1 and Figure 3.Only ^{235}U fuel is used, no fuel salt is

*e-mail: yanrui@sinap.ac.cn

added during operation, and all fuel salts are completely unloaded at the EOL.

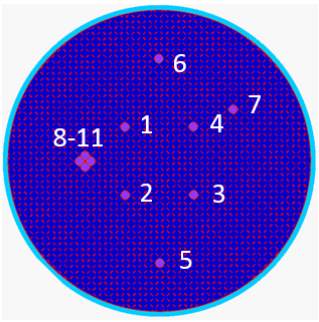

Figure 1. Reactor core model(Top view)

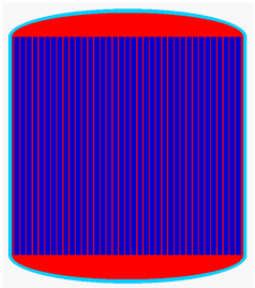

Figure 2. Reactor core model(Side view)

Table 1. Overall design parameters of 2MW MSR

Thermal power \ MW	2
Full power operation days \ d	300
Average Power Density of Fuel \ MWm^{-3}	1.27
life \ a	10
Reactor inlet outlet temperature \ $°C$	600 650
Fuel salt	$LiF - BeF_2 - UF_4$
	65.3% – 28.71% – 4.79% – 1.20%
Fuel salt density \ gcm^{-3}	2.31
Uranium fuel enrichment \ wt%	19.75
Flow rate of primary loop \ $cm^3 s^{-1}$	2.24×10^4
moderator material	Graphite

The mathematical model established is shown in equation (1)

$$\frac{dN_{i,j}[t]}{dt}=\sum_{k=1}^{n}\gamma_{k,i}\sigma_{k,f,j}N_{k,j}[t]\phi_j+\sum_{k=1}^{n}\sigma_{k\to i}N_{k,j}[t]\phi_j+\sum_{k=1}^{n}b_{k\to i}\lambda_k^{dec}N_{k,j}[t]$$
$$-\sigma_{i,j,f}N_{i,j}[t]\phi_j-(\sigma_{i,j}-\sigma_{i,f,j})N_{i,j}[t]\phi_j-\lambda_i^{dec}N_{i,j}[t]+\sum_{m=1}^{a}\lambda_{i,m\to j}^{flowin}N_{i,m}[t]$$
$$-\sum_{m=1}^{a}\lambda_{i,j\to m}^{flowout}N_{i,j}[t] \quad (1)$$

Among them:

n=1,...,i,..., Represents the type of nuclide to be solved;

a=1,...,j,..., Represents the number of areas divided for the primary loop system;

$N_{i,j}[t]$, Represents the atomic density of nuclide i in region j;

$\gamma_{k,i}$, Represents fission yields of nuclide k fission to nuclide i;

$\sigma_{k,f,j}$, Represents the fission reaction cross section of nuclide k in the region j;

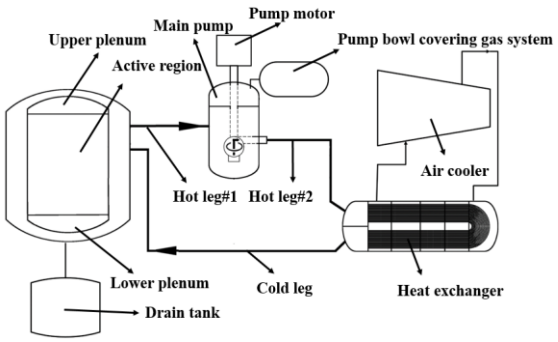

Figure 3. Schematic diagram of 2MW MSR system

Table 2. Verification of static burnup simulation results with ORIEGNS \ Bq

Nuclide	Half life(s)	ORIGEN-S	Mathematica	deviation \ %
^{83m}Kr	6.59×10^3	3.38×10^{14}	3.54×10^{14}	4.80
^{85m}Kr	1.61×10^4	7.92×10^{14}	8.52×10^{14}	7.57
^{85}Kr	3.40×10^8	9.52×10^{12}	9.37×10^{12}	-1.55
^{87}Kr	4.58×10^3	1.61×10^{15}	1.66×10^{15}	3.11
^{88}Kr	1.02×10^4	2.20×10^{15}	2.24×10^{15}	1.74
^{131m}Xe	1.03×10^6	1.97×10^{13}	2.06×10^{13}	4.53
^{133m}Xe	1.89×10^5	1.23×10^{14}	1.29×10^{14}	4.98
^{133}Xe	4.53×10^5	4.05×10^{15}	4.43×10^{15}	9.25
^{134m}Xe	2.90×10^{-1}	2.18×10^{13}	2.11×10^{13}	-3.25
^{135m}Xe	9.18×10^2	7.34×10^{14}	6.85×10^{14}	-6.66
^{134m}Xe	3.29×10^4	3.81×10^{15}	3.87×10^{15}	1.63
^{138}Xe	8.45×10^2	3.94×10^{15}	4.16×10^{15}	5.40

$\sigma_{i.j}$, Represents the microscopic cross section of nuclear reactions except fission reactions of nuclide i in the region j;

ϕ_j, Represents the neutron flux density in the region j;

$\sigma_{k\to i,j}$, Represents the microscopic cross section of nuclide i is produced by the nuclear reaction of nuclide k in region j;

$b_{k\to i}$, Represents the decay branching ratio of nuclide k to nuclide i;

λ_i^{dec}, Represents decay constant of nuclide i;

3 Results and Discussion

3.1 Numerical verification

The krypton and xenon activity under static condition (flow rate = 0) was calculated and compared with ORIGEN-S as shown in Table 2. It can be seen that the deviation is less than 10%. It was preliminarily verified that the mathematical model and the nuclear data are reliable.

3.2 Flowing state simulation results

The distribution of krypton and xenon source term at EOL under rated flow rate(flow rate = $22400cm^{3-1}$) is shown in Table 3 without considering online removal. It can be seen that under normal operation conditions, the total activity of krypton and xenon in primary loop system is as follows: core: 8.11×10^{15}Bq (44.1%), Upper plenum: 5.25×10^{15}Bq (28.5%), hot leg1:

2.13×10^{14}Bq (1.16%), main pump: 3.43×10^{15}Bq (18.6%) , Hot leg2: 2.13×10^{14}Bq (1.15%) , heat exchanger: 5.48×10^{14}Bq(2.97%), Cold leg: 4.25×10^{14}Bq (2.31%), Lower plenum: 2.20×10^{14}Bq(1.19%).

The dynamic analysis program in this work can accurately simulate the evolution of krypton and xenon concentration inside and outside the core after the reactor start-up. The figure 4 and figure 5 shows the variation of krypton xenon concentration inside and outside the core with start-up time at rated flow rate (flow rate = 22400 cm^3s^{-1}). It can be seen that krypton and xenon begin to accumulate instantaneously at the beginning of fission reaction in the reactor. Due to the flow effect of fuel salts, there is a time lag in the change of the concentration of krypton and xenon outside the core at the initial stage of reactor start-up. After about sixty seconds, the concentration of krypton and xenon outside the core will tend to be the same with that inside the core.Obviously, the time required for the concentration of krypton and xenon outside the core tend to be the same as the concentration inside the core is comparable to the time required for one cycle of fuel salt in primary loop.

The figure 6 and figure 7 shows the variation of krypton xenon concentration inside and outside the core with start-up time at low flow rate (flow rate = 224 cm^3s^{-1}). It can be seen that the time required for the concentration of krypton and xenon outside the core tend to be the same as the concentration inside the core will be greatly increased.The main reason is that some short-lived nuclides will decay rapidly after they flow out of the core, and the concentration of these nuclides inside and outside the core will no longer be the same.As long-lived nuclides accumulate gradually, their concentration gradually accounts for the main contribution at the EOL, so the concentration of krypton and xenon inside and outside the core gradually tend to be the same after a long time, which is obviously longer than the time required for one cycle of fuel salt in primary loop.

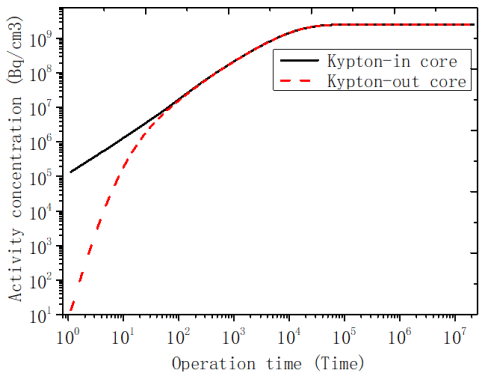

Figure 4. Krypton concentration in and out of the core varies with time after start-up

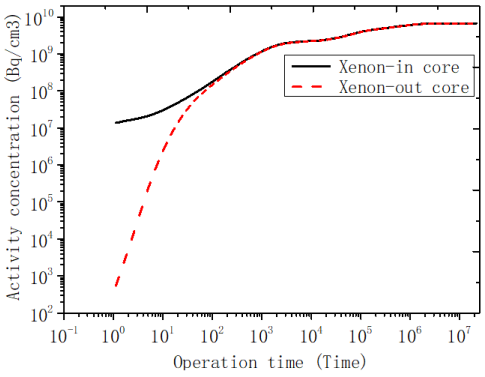

Figure 5. Xenon concentration in and out of the core varies with time after start-up

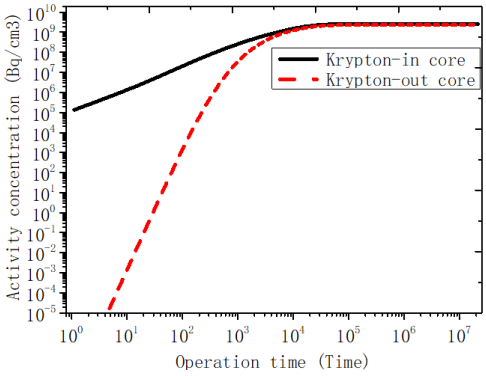

Figure 6. Krypton concentration in and out of the core varies with time after start-up

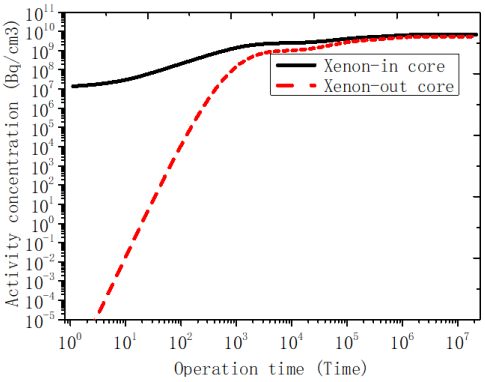

Figure 7. Xenon concentration in and out of the core varies with time after start-up

3.3 krypton and xenon in off-gas system

Figure shows the activity curves of krypton and xenon in the off-gas system with different removal fractions. It can be seen that the activity of krypton and xenon isotopes in the off-gas system increases gradually with the increase of removal fraction and tends to the maximum accumulated value, except for ^{135}Xe. Compared with the dynamic model, the static burnup model underestimated the total activity of ^{135}Xe by 6.61%. This is mainly due to the timely removal of ^{135}Xe from the primary loop system and no longer being captured and absorbed by neutrons.The

Table 3. Activity distribution of krypton, xenon and iodine in the primary Loop at the EOL \ Bq

Nuclide	Core	Upper plenum	Hot leg1	Main pump	Hot leg2	Heat exchanger	Cold leg	Lower plenum
^{83m}Kr	1.56×10^{14}	1.01×10^{14}	4.10×10^{12}	6.60×10^{13}	4.09×10^{12}	1.06×10^{13}	8.18×10^{12}	4.22×10^{12}
^{85m}Kr	3.75×10^{14}	2.43×10^{14}	9.86×10^{12}	1.59×10^{14}	9.85×10^{12}	2.54×10^{13}	1.97×10^{13}	1.02×10^{13}
^{85}Kr	4.13×10^{12}	2.67×10^{12}	1.08×10^{11}	1.75×10^{12}	1.08×10^{11}	2.80×10^{11}	2.17×10^{11}	1.12×10^{11}
^{87}Kr	7.31×10^{14}	4.73×10^{14}	1.92×10^{13}	3.10×10^{14}	1.92×10^{13}	4.95×10^{13}	3.84×10^{13}	1.98×10^{13}
^{88}Kr	9.85×10^{14}	6.37×10^{14}	2.59×10^{13}	4.17×10^{14}	2.59×10^{13}	6.68×10^{13}	5.17×10^{13}	2.67×10^{13}
^{131m}Xe	9.08×10^{12}	5.87×10^{12}	2.39×10^{11}	3.85×10^{12}	2.39×10^{11}	6.16×10^{11}	4.77×10^{11}	2.46×10^{11}
^{133m}Xe	5.67×10^{13}	3.66×10^{13}	1.49×10^{12}	2.40×10^{13}	1.49×10^{12}	3.84×10^{12}	2.98×10^{12}	1.54×10^{12}
^{133}Xe	1.95×10^{15}	1.26×10^{15}	5.12×10^{13}	8.26×10^{14}	5.12×10^{13}	1.32×10^{14}	1.02×10^{14}	5.29×10^{13}
^{134m}Xe	1.25×10^{13}	8.13×10^{12}	1.25×10^{11}	7.26×10^{10}	1.70×10^{9}	8.31×10^{8}	1.50×10^{8}	2.15×10^{11}
^{135m}Xe	3.02×10^{14}	1.95×10^{14}	7.93×10^{12}	1.28×10^{14}	7.93×10^{12}	2.05×10^{13}	1.59×10^{13}	8.19×10^{12}
^{135}Xe	1.70×10^{15}	1.10×10^{15}	4.47×10^{13}	7.21×10^{14}	4.47×10^{13}	1.15×10^{14}	8.95×10^{13}	4.62×10^{13}
^{138}Xe	1.83×10^{15}	1.19×10^{15}	4.83×10^{13}	7.73×10^{14}	4.79×10^{13}	1.23×10^{14}	9.55×10^{13}	4.93×10^{13}
Total	8.11×10^{15}	5.25×10^{15}	2.13×10^{14}	3.43×10^{15}	2.13×10^{14}	5.48×10^{14}	4.25×10^{14}	2.20×10^{14}
percent	44.1%	28.5%	1.16%	18.6%	1.15%	2.97%	2.31%	1.19%

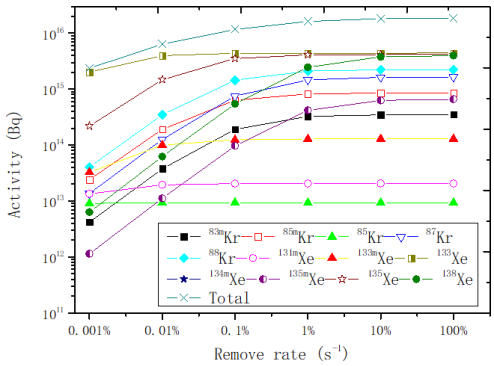

Figure 8. Krypton and xenon in off gas system with removal fractions

activity(1.63×10^{16}Bq) of krypton-xenon isotopes in the off-gas system tends to the maximum accumulation value (1.84×10^{16}Bq, of which ^{83m}Kr, ^{85m}Kr, ^{87}Kr, ^{88}Kr, ^{133}Xe, ^{135}Xe and ^{138}Xe account for about 95.6%) when the removal fraction is more than 1%. Because the fission reactor continues to occur in the core and krypton and xenon can only be removed when they flow through the main pump, there are still 2.64×10^{14}Bq, of which ^{138}Xe, ^{135m}Xe, ^{134m}Xe, ^{87}Kr and ^{83m}Kr account for about 93.6% krypton and xenon remain in the primary loop system, with the removal fraction of 100%.

4 Discussion

In this work, a numerical model of krypton and xenon for the primary loop and off-gas system of molten salt reactor was established based on Mathematica.Preliminary validation with ORIGEN-S program in SCALE 6.1 package shows that the deviation of the results under static burnup is less than 10%, which indicates that the analysis method and the nuclear database used are reasonable and reliable.The numerical model has strong universality and can be used to analyze krypton and xenon source terms of different molten salt reactors or even solution reactors, according to different input power, volume, flow rate or removal fraction parameters. The conclusions obtained provide a reference for the safety management of krypton and xenon radioactive sources in off-gas system in 2MW MSR.

Acknowledgments

This work was supported by the Chinese Academy of Sciences TMSR Strategic Pioneer Science and Technology Project (No.XDA02010000) and Thorium uranium fuel cycle characteristics andkey problem research Project (No. QYZDY-SSW-JSC016).

References

[1] Cottrell W B, Hungerford H E, Leslie J K, et al. Operation of the aircraft reactor experiment[R]. USA: ORNL (1955)

[2] Briant. Collection of papers on the aircraft reactor experiment, Nuclear Science and Engineering **2**, 797-853 (1957)

[3] Weinberg A M, Rosenthal M W, Haubenreich P N, et al. Collection of papers on the molten salt reactor experiment, Nuclear Application Technology **8**, 105-219 (1970)

[4] Scott D, Grindell A G. Components and systems development for molten-salt breeder reactors, ORNL-TM-1855[R]. USA: ORNL, (1967)

[5] Robertson R C, Smith O L, Briggs R B. Two fluid molten-salt breeder reactor design study, ORNL-4528[R]. USA: ORNL, (1970)

[6] Robertson R C. Conceptual design study of a single fluid molten-salt breeder reactor, ORNL-4541[R]. USA: ORNL, (1971)

[7] Engel J, Bauman H, Dearing J, et al. Conceptual design characteristics of a denatured molten-salt reactor with once-through fueling[R]. USA: ORNL, (1980)

[8] JIANG Mianheng, XU Hongjie, DAI Zhimin. Advanced nuclear fission energy-nuclear energy system. nuclear energy system **27**, 366-374 (2012)